

# Interference-Free Measurements of the Subsonic Aerodynamics of Slanted-Base Ogive Cylinders

Colin P. Britcher\* and Charles W. Alcorn†  
Old Dominion University, Norfolk, Virginia 23529

Drag, lift, pitching moment, and base-pressure measurements have been made, free of support interference, on a range of slanted-base ogive cylinders, using the NASA Langley Research Center 13-in. magnetic suspension and balance system. Test Mach numbers were in the range 0.04–0.2. Two types of wake flow were observed, a quasisymmetric turbulent closure or a longitudinal vortex flow. Aerodynamic characteristics differ dramatically between the two wake types. Drag measurements are shown to be in agreement with previous tests. A hysteretic behavior of the wake with varying Reynold's number has been discovered for the 45-deg base. An interaction between forebody boundary-layer state and wake flow and base pressures has been detected for higher slant angles.

## Nomenclature

$C_L$	= lift coefficient, based on frontal area
$C_D$	= drag coefficient, based on frontal area
$C_M$	= pitching moment coefficient, based on frontal area and half length of 0-deg base model
$Re_D$	= Reynold's number, based on model diameter
SCR	= silicon controlled rectifier

## Introduction

SLANTED-BASE ogive-cylinder models have been tested by Morel<sup>1,2</sup> and others.<sup>3,4</sup> The principal interest in this geometry is the sudden change of wake structure, with corresponding large change in drag coefficient, occurring for small changes of base slant angle, around 45-deg slant. The two wake types are a quasisymmetric, turbulent closure at low slant angles and a longitudinal vortex flow at high slant angles, illustrated in Fig. 1. The original application of these tests was as an analogy to the flow over the sloping rear windows of hatchback and fastback automobiles as illustrated in Fig. 2. For the work reported here, the model is conceptually "inverted" and argued to be an analogy to the flow under the upswept rear fuselage of a transport aircraft. Design constraints are similar in both cases—namely, minimum drag and maximum utilization of enclosed volume. The former tends to suggest slender, tapering bases while the latter suggests rather blunt geometries. Rather perversely, automobiles commonly show minimum drag with a blunt base. This is due to the formation of intense trailing vortices from the corners of the sloping rear window of fastback designs, leading to high induced drag.

Of particular relevance to the aircraft application, it has already been shown that the vortical wake is completely disrupted by introduction of a conventional rear support sting,<sup>5</sup> leading to large discrepancies between interference-free and sting-supported measurements. The discrepancy in drag coefficient can be as much as a factor of two. It is also noted that analytic or numerical methods capable of accounting for these discrepancies have not been demonstrated, due to the presence of a large and difficult separated flow region.

## Experimental Details

The models used<sup>5,6</sup> correspond to Morel's geometry and are illustrated in Fig. 3. The models are manufactured from aluminum alloy, with enclosed low-carbon iron cores. Considerable care was taken to ensure geometric fidelity and high quality of surface finish. Interchangeable bases cover a range of base slant angles (0, 30, 40, 45, 50, 60, and 70 deg). One model is used exclusively for force and moment tests, while an alternate, of nominally identical aerodynamic lines, is equipped for direct measurement of base pressures. Model mass varied, depending on base and equipment fitted but was typically just less than 1 kg. For all tests, the models are suspended magnetically with no mechanical support of any kind. Previous magnetically suspended tests with these models have established

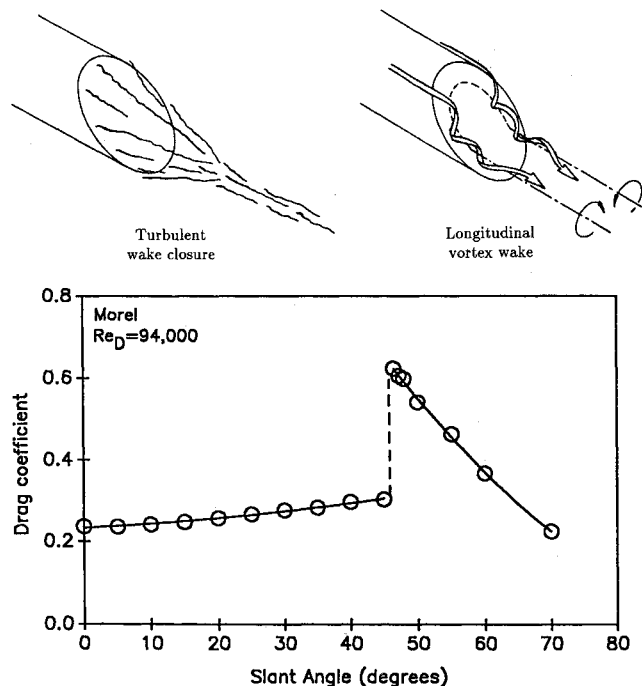


Fig. 1 Slanted-base ogive-cylinder aerodynamics.

Received March 23, 1990; revision received June 8, 1990; accepted for publication June 11, 1990. Copyright © 1990 by the American Institute of Aeronautics and Astronautics, Inc. All rights reserved.

\*Assistant Professor, Department of Mechanical Engineering and Mechanics. Member AIAA.

†Graduate Research Assistant. Student Member AIAA.

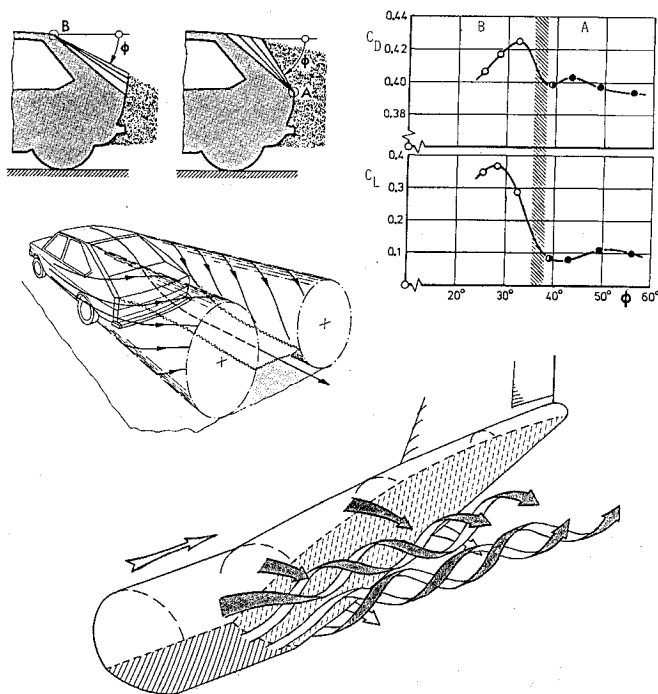


Fig. 2 Slanted-base aerodynamics: automobile (upper) and aircraft fuselage (lower).

their basic aerodynamic characteristics and are fully reported elsewhere.<sup>5,6</sup>

The NASA Langley Research Center 13-in. magnetic suspension and balance system (MSBS) has been developed from a system constructed at the Arnold Engineering Development Center in the 1960's,<sup>7</sup> although little of the original hardware remains in use. The position and attitude of the model is detected optically<sup>8</sup>; position signals are fed to a digital control system<sup>9</sup> with the electromagnet currents supplied by bipolar SCR power amplifiers. The wind tunnel is a low-speed, open circuit design,<sup>10</sup> illustrated in Fig. 4, with a maximum Mach number of 0.5. An aluminum alloy dummy sting and support strut can be installed downstream for support-interference evaluations.

Base pressures can be measured using a single-channel on-board pressure telemetry system.<sup>11</sup> For these tests, a 2 psi, piezo-resistive, differential transducer was installed in the base of the model, referenced to a total pressure tap in the extreme nose, barely visible in Fig. 3. The transducer output is amplified, encoded as an FM signal, and transmitted out from the model by an IR LED. Base pressures are therefore derived from the difference between base static and tunnel total pressure compared to the difference between local static and tunnel total.

Models were suspended close to the centerline of the wind tunnel, at nominally zero angles of attack and sideslip. The "clean" model is thought to exhibit principally laminar boundary layers, with transition just beginning to move forward from the base at the higher Reynolds numbers tested. Maximum Mach numbers (typically 0.2) were well below the tunnel limit (0.5), mostly due to problems with the electromagnet power supplies. Most tests were repeated with transition fixed 2 cm downstream of the ogive-cylinder junction by a ring of no. 60 grit. Some check runs were made with coarser grit to ensure tripping at lower Reynolds numbers.

Three separate test sequences were run:

1) Magnetically suspended. Electromagnet currents recorded as a function of tunnel speed.

2) Magnetically suspended with base-pressure telemetry. One pressure was recorded as a function of tunnel speed, the tunnel stopped for change of pressure tap, and the process repeated. Base-pressure data have only been taken for base slant angles of 0, 40, 45, and 50 deg due to the laborious test-

ing procedure required with the single-channel telemetry system.

3) Magnetically suspended with dummy sting. The rear portion of the model was modified to provide a representative sting cavity and was then magnetically suspended with a dummy sting protruding into the cavity, but not in contact with any portion of the model. Sting interferences are the primary focus of a separate report.<sup>5</sup>

### Calibration and Data Reduction

Aerodynamic forces and moments are deduced from electromagnet current measurements. Analysis has shown<sup>6</sup> that the drag and lift forces and pitching moment acting on a model at zero angles of attack and sideslip in the 13-in. MSBS can be expressed as a nonlinear function of electromagnet currents. The "nonlinearity" is simply a square-law relationship between currents and forces or moments, which arises due to the use of a freely magnetized iron core in the suspended model and not due to any saturation effects. The coefficients in the calibration equations are found by multiple regression fitting of wind-off calibration data, obtained from a calibration model, magnetically suspended and loaded at three stations.

Electromagnet currents, typically around 20 A (each) to suspend a model, can be resolved to around  $\pm 10$  mA, resulting in typical uncertainties in drag force of around  $\pm 0.002$  N, lift force of around  $\pm 0.015$  N, and pitching moment of around  $\pm 0.001$  Nm. This is compared to a model weight of close to 10 N and maximum drag forces in this test program of roughly 1.3 N. However, it must be stated that the calibration procedures employed are still under development and rigorous

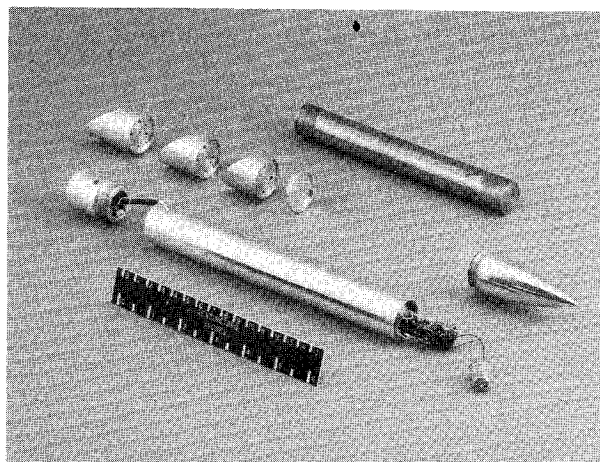
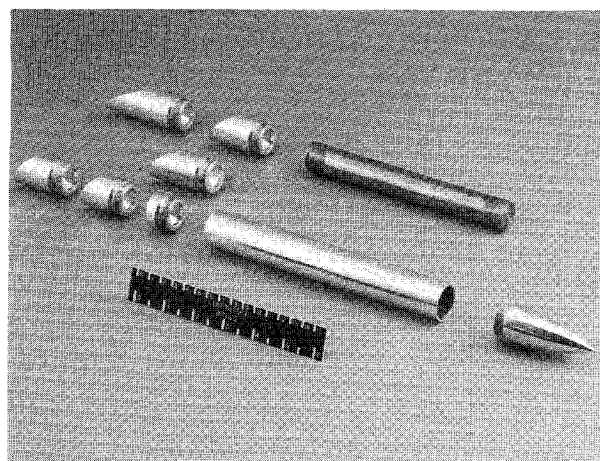


Fig. 3 Force model (upper) and pressure model (lower).

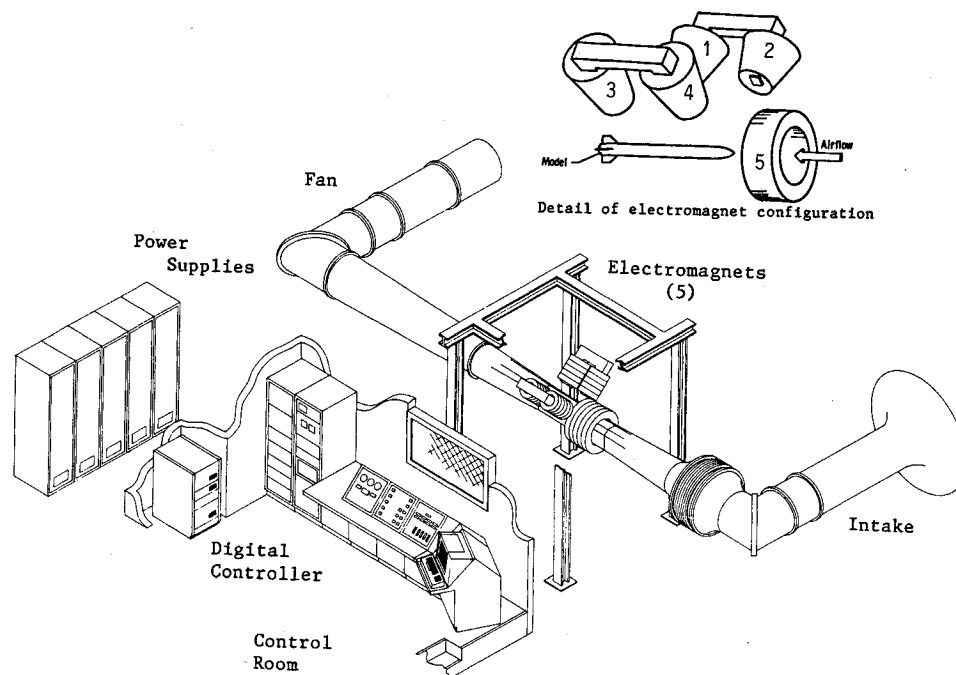


Fig. 4 NASA Langley 13-in. MSBS laboratory.

assessment of the accuracy of the derived calibration coefficients and the implications of any inaccuracy has not been perfected. Error bars are included on the first drag and the first lift and pitching moment plots as a guide. It is clear that the uncertainty is serious at the lowest speeds, but appears to be rather small at the higher tunnel speeds. The magnitudes of the aerodynamic effects being studied are so large, however, that there can be little doubt that the magnitudes and trends are properly represented.

Tunnel Mach number is derived from pressure measurements in a conventional manner and is considered accurate to  $\pm 0.1\%$ . Mach number and drag-force corrections have been applied to account for model and wake blockage and longitudinal buoyancy (pressure gradient), following classical methods.<sup>5,6</sup> Base pressures have been corrected for model blockage and longitudinal pressure gradients. Lift forces are nondimensionalized by the model cross-sectional area. Pitching moments are nondimensionalized using the same reference area and the half-length of the zero-degree base model. These choices result in large numeric values of  $C_L$  and  $C_M$ , although the forces and moments involved are typically quite small.

#### Aerodynamics Results: Low Base Slant Angles

Drag coefficients for the zero-degree base are shown in Fig. 5. Slight reductions in drag coefficients with increasing Reynold's number are noticeable, particularly for the fixed transition cases consistent with usual boundary-layer behavior. Similar behavior for the 30- and 40-deg bases is shown in Fig. 6. The wake structure for all these models is a quasymmetric turbulent closure.

Base pressures for the zero-degree base appear quite uniform over the base, as commonly expected. The 40-deg base exhibits significant nonuniformities, as illustrated in Fig. 7. The nonuniformity is most noticeable along the plane of symmetry and is due to the external flow turning so as to flow somewhat down the plane of the base, i.e., from Port #8 toward Port #10 in Fig. 7. There is slight evidence that differences may exist between free and fixed transition cases. Lift and pitching moments for the 40-deg base, shown in Fig. 8, indicate relatively constant values of  $C_L$  and  $C_M$  with varying Reynold's number. This is due to the fact that base pressures are the primary contribution to all aerodynamic forces and

moments and they, in turn, are relatively constant with Reynold's number. It is worthy of note that the lift forces in this case are extremely small, between 0.2% and 6% of the model's weight.

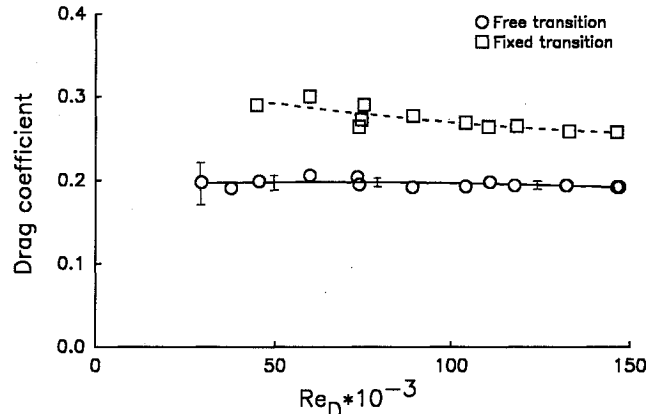


Fig. 5 Zero-degree base, drag coefficients.

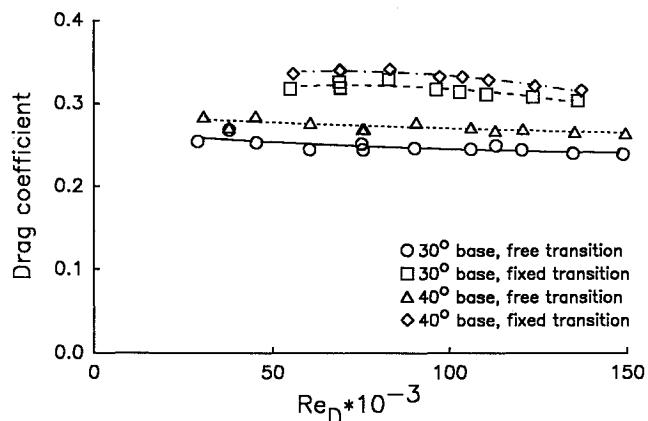


Fig. 6 30- and 40-deg base, drag coefficients.

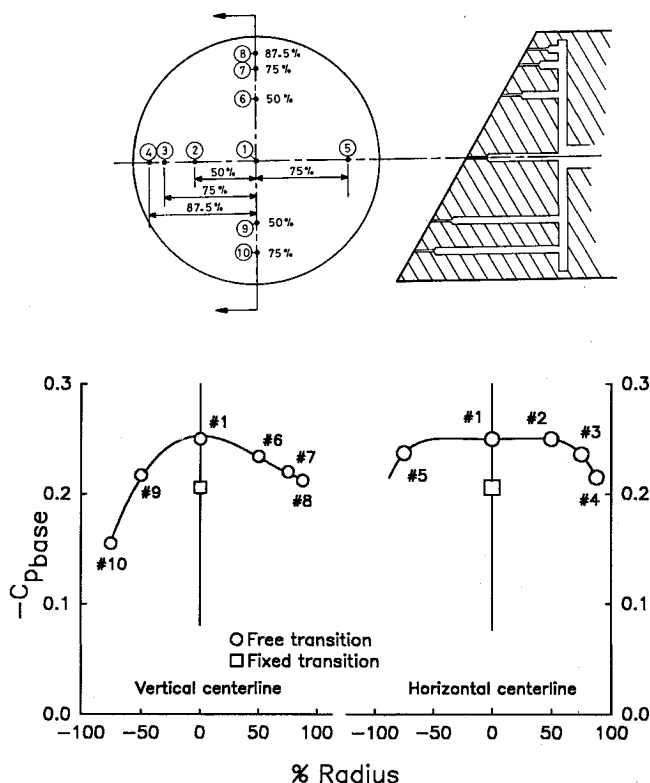
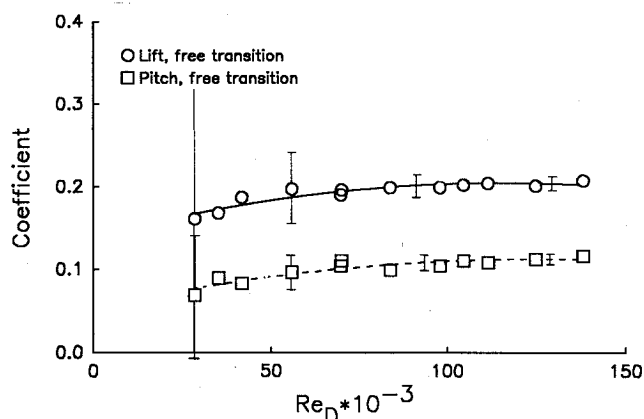
Fig. 7 40-deg base, base-pressure distribution,  $Re_D = 94,000$ .

Fig. 8 40-deg base, lift and pitching moment coefficients.

#### 45-Degree Base

With free transition (laminar boundary layers), the wake structure at low Reynold's numbers is a quasisymmetric turbulent closure, characteristic of lower slant angles. As  $Re_D$  is increased past 60,000 or so, the wake structure suddenly changes to a longitudinal vortex flow, characteristic of higher slant angles. The associated change in drag is dramatic, more than a doubling in value. Furthermore, once the vortex flow is established, it persists even as  $Re_D$  is reduced below the "critical" value, leading to a substantial hysteresis in drag coefficient, evident in Fig. 9. The effect is very repeatable and occurs at the same Reynold's number for both force and pressure models. A hysteretic behavior of vortical wakes with changing model angle of attack was observed by Morel<sup>1</sup> and later suspected by Maull.<sup>4</sup> The present results, although at zero angle of attack, are presumed to arise from the same mechanism, that is, complete stability of two different wakes on the same model under the same conditions.

It is believed, although not yet experimentally confirmed, that the changes in wake structure with varying Reynold's number are linked with the onset of natural transition at the model's base or in the free shear layers developing just down-

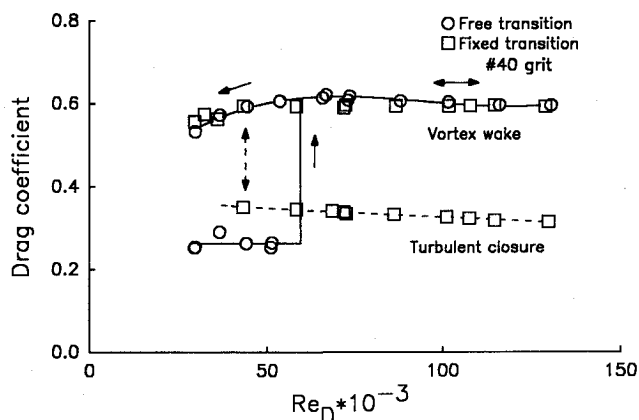


Fig. 9 45-deg base, drag coefficients.

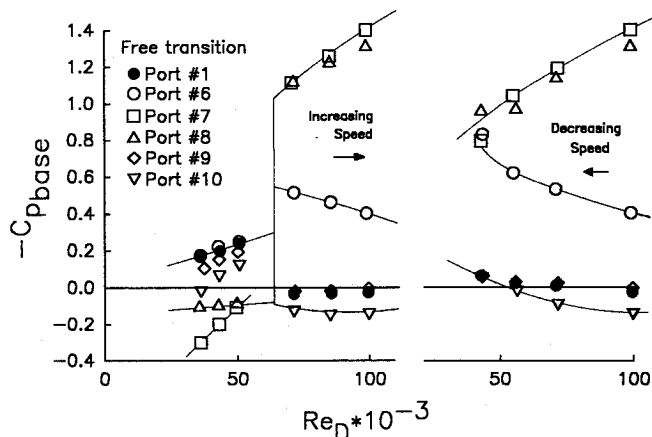
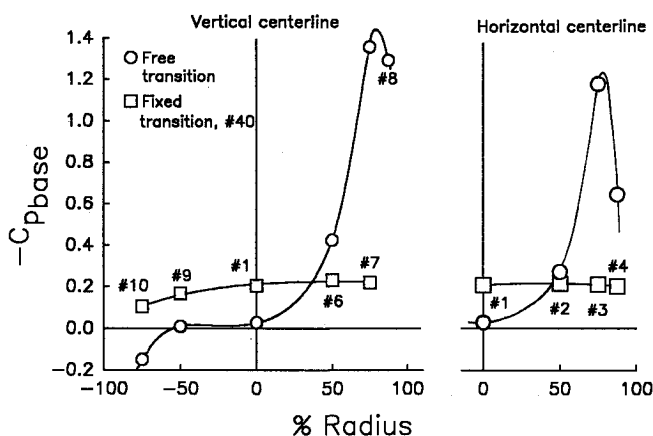


Fig. 10 45-deg base, base-pressure coefficients.

Fig. 11 45-deg base, base-pressure distribution,  $Re_D = 94,000$ .

stream. The fact that the effect had not previously been detected is thought to be due to boundary-layer tripping by upstream wire attachments,<sup>6</sup> preventing development of the wake from an initially laminar shear layer.

With transition fixed (turbulent boundary layers), the change in wake structure is inhibited. With a coarse grit size (#40), ensuring transition at the lower Reynold's numbers, the wake remains a quasisymmetric closure and the drag coefficient remains low. It happens that the smaller grit size normally employed (#60) is marginally effective in tripping the boundary layer below  $Re_D$  of 60,000. Under these conditions, repeat sweeps up and down through the "critical" Reynold's number sometimes exhibit the wake structure change, sometimes not. Furthermore, spontaneous reorganization of

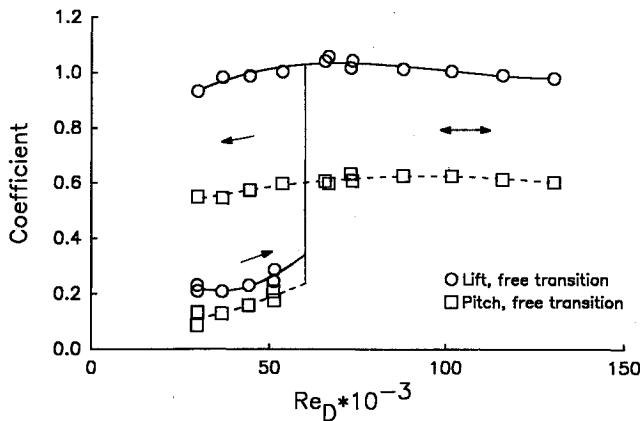


Fig. 12 45-deg base, lift and pitching moment coefficients.

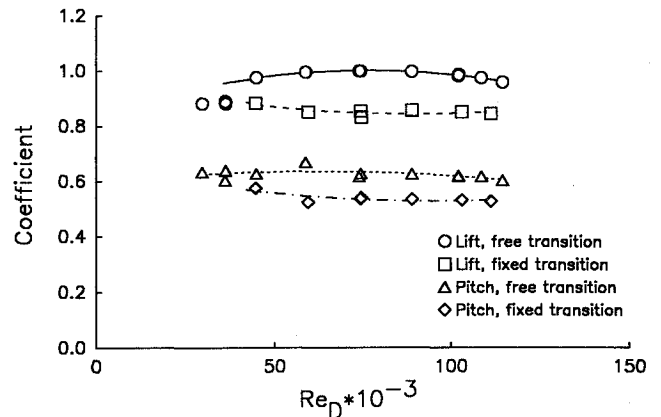


Fig. 15 50-deg base, lift and pitching moment coefficients.

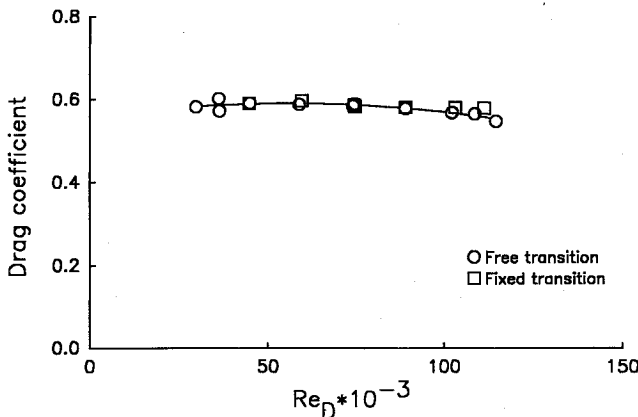
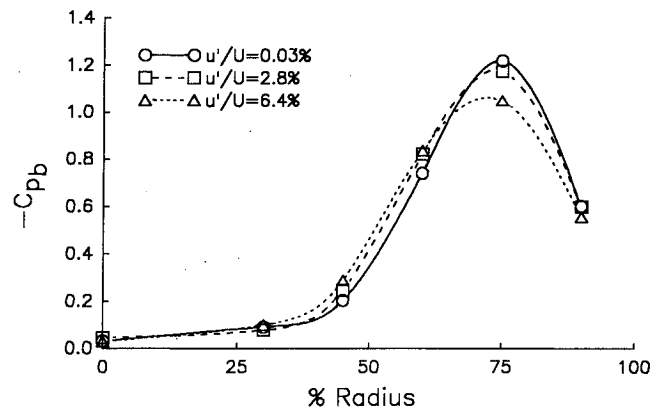
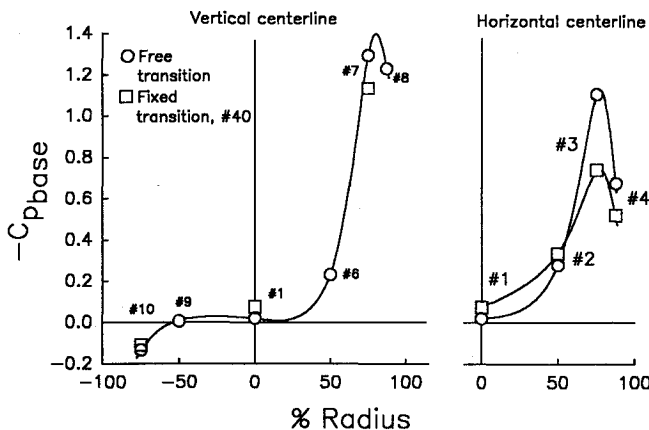
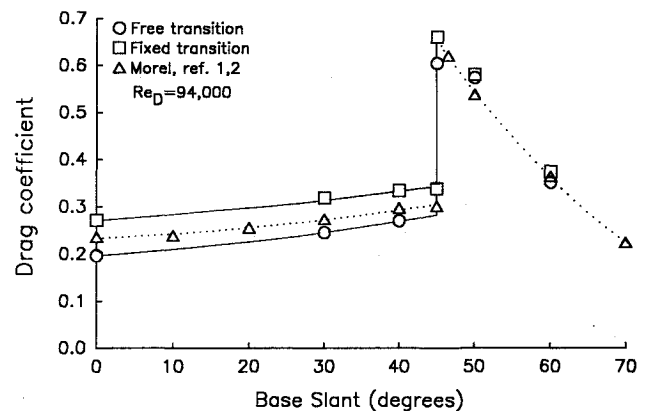


Fig. 13 50-deg base, drag coefficients.

Fig. 16 Effect of freestream turbulence on base pressures, 50-deg base (Ref. 3),  $Re_D = 200,000$ .Fig. 14 50-deg base, base-pressure distribution,  $Re_D = 94,000$ .Fig. 17 Drag coefficient vs base slant angle,  $Re_D = 94,000$ .

the wake has been observed below the critical Reynold's number, although never above.

The free transition base pressures for the 45-deg base, shown in Fig. 10, dramatically illustrate the wake hysteresis. The apparently steep variations of pressure coefficients with Reynold's number above the critical value are thought to be genuine, but may be due to slight shifts in the vortex locations, rather than changes in strength or structure. Data below the critical Reynold's number should be considered unreliable, due to the very small pressure differences encountered. Figure 11 illustrates the distinctive pressure "footprint" of the vortices, with high suctions in the region of the vortex cores. This type of pressure distribution has been reported in previous studies<sup>1,3</sup> and arises due to the "horseshoe" pattern adopted by the vortex loop on the surface of the base, as depicted ear-

lier in Fig. 1. If the strength of the vortex was roughly constant along its length, the results imply that the vortex lies closest to the surface at the upstream end of the base.

Pressure measurements confirm that boundary-layer tripping inhibits the formation of the vortical wake, nevertheless again showing substantial nonuniformities, also seen in Fig. 11. Lift and pitching moment results, shown in Fig. 12, again show the characteristic hysteretic behavior of the wake.

### High Slant Angles

The wake for high slant angles is a longitudinal vortex flow. Drag coefficients for the 50-deg base are shown in Fig. 13. It should be noted that the increment in drag between fixed and free transition runs, consistently observed for the lower slant angles, is not repeated at higher slant angles. Since there must

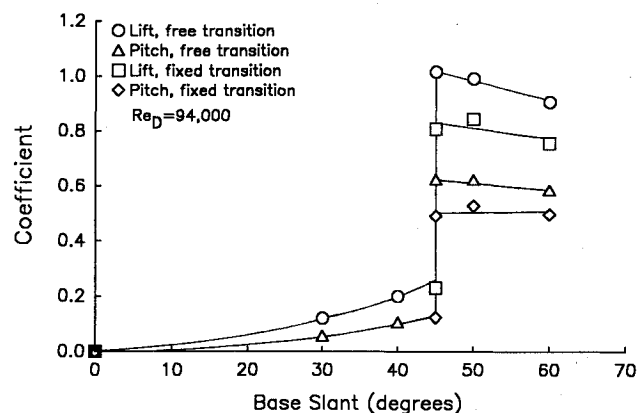


Fig. 18 Lift and pitching moment coefficient vs base slant angle,  $Re_D = 94,000$ .

be an increment (increase) in forebody skin friction, suspicions are aroused as to whether the base drag changes by a similar increment, but in the opposite sense. Base pressures for the 50-deg base, shown in Fig. 14, clearly confirm this idea, showing significantly higher (less negative) values in the region of the vortices with fixed transition. Lift forces and pitching moments are presumed to depend largely on base pressures and are relatively independent of forebody drag, hence show clear differences between free and fixed transition runs, seen in Fig. 15, confirming that the wake vortices weaken with transition fixed.

The effect of freestream turbulence on wake flow was studied by Xia and Bearman.<sup>3</sup> A strong influence on the vortical wake was detected, specifically an apparent weakening of wake vortices, with relatively little effect on the quasisymmetric wake. This is illustrated in Fig. 16. The similarity to Fig. 14 is striking. It is suggested that the change in vortex strength may be driven by more rapid breakup or by increased mixing in the free shear layers just downstream of the base. Thus, turbulence impinging from the freestream or being convected into the wake by the forebody boundary layer would have similar influences.

Additional data were taken for a 60-deg base and is included in the summary plots.

### Discussion

Figure 17 shows a comparison of interference free drag coefficients to the original data by Morel<sup>1</sup> ( $Re_D = 94,000$ ). MSBS points are obtained by interpolation for each base slant. Agreement for the interference free cases is quite good at the higher slant angles. At the lower slant angles, it is supposed that partial boundary-layer tripping was induced by Morel's wire supports,<sup>6</sup> leading to a value for forebody drag lying between the fixed and free transition MSBS values. The critical slant angle was fractionally lower in the MSBS tests than had been previously reported. The convergence of all results above the critical slant angle is again notable.

Lift and pitching moment measurements, summarized in Fig. 18, are broadly consistent with drag results, although vortical wakes are more clearly seen to be sensitive to the state of the oncoming boundary layer. The lift and pitching moment coefficients stay rather high as the base angle is increased beyond 45 deg, whereas the drag coefficients were seen to fall

rapidly. This is due to the combination of a reduction in vortex strength as slant angle increases, together with a projection of progressively more base slant area in the "lift" direction (perpendicular to the freestream).

The hysteretic behavior of the wake for the 45-deg base is an interesting phenomena, worthy of further study. The extensive data base now available for slanted-base ogive-cylinder geometries is suggested as a possible bench mark for drag prediction or support-interference correction methods.

### Conclusions

Previous measurements of drag and base pressures for slanted-base ogive cylinders have been validated and extended to include lift forces and pitching moments. The dramatic change in aerodynamic characteristics corresponding to the wake structure change around 45-deg slant has been confirmed. A hysteretic behavior of the vortical wake with changing Reynolds number has been discovered for the 45-deg base. It has also been shown that the strength of wake vortices is influenced by the state of the forebody boundary layer. The 13-in. MSBS has been shown, for the first time, to be capable of measuring combined lift, drag, and pitching moments.

### Acknowledgments

This work was partially supported by NASA Langley Research Center under Grant NAG-1-716, Richmond P. Boyden, technical monitor.

### References

- Morel, T., "Effect of Base Slant on the Flow Patterns and Drag of Three-Dimensional Bodies with Blunt Ends," *Symposium on Aerodynamic Drag Mechanisms of Bluff Bodies and Road Vehicles*, Sept. 1976, Plenum, New York, 1978, pp. 191-226.
- Morel, T., "Aerodynamic Drag of Bluff Body Shapes Characteristic of Hatch-Back Cars," *SAE Congress and Exposition*, Society of Automotive Engineers, Detroit, MI, March 1978, Paper 780267.
- Xia, X. J., and Bearman, P. W., "An Experimental Investigation of the Wake of an Axisymmetric Body with a Slanted Base," *Aeronautical Quarterly*, Vol. 43, Feb. 1983, pp. 24-45.
- Mauil, D. J., "The Drag of Slant-Based Bodies of Revolution," *Aeronautical Journal*, Vol. 84, No. 833, June 1980, pp. 164-166.
- Britcher, C. P., Alcorn, C. W., and Kilgore, W. A., "Subsonic Sting Interference on the Aerodynamic Characteristics of a Family of Slanted-Base Ogive Cylinders," NASA CR-4299, June 1990.
- Alcorn, C. W., "An Experimental Investigation of the Aerodynamic Characteristics of Slanted-Base Ogive Cylinders Using Magnetic Suspension Technology," NASA CR-181708, Sept. 1988.
- Boyden, R. P., Britcher, C. P., and Tchong, P., "Status of Wind-Tunnel Magnetic Suspension Research," Society of Automotive Engineers, TP-851898, Oct. 1985.
- Tchong, P., and Schott, T. D., "A five-component electro-optical positioning system," *ICIASF '87 Record*, June 1987, pp. 322-333.
- Britcher, C. P., Goodyer, M. J., Eskins, J., Parker, D., and Halford, R. J., "Digital Control of Wind-Tunnel Magnetic Suspension and Balance Systems," *ICIASF '87 Record*, June 1987, pp. 334-342.
- Johnson, W. G., and Dress, D. A., "The 13-inch Magnetic Suspension and Balance System Wind Tunnel," NASA TM-4090, Jan. 1989.
- Tchong, P., and Schott, T. D., "A Miniature Infrared Pressure Telemetry System," *Proceedings of the 34th International Instrumentation Symposium*, Albuquerque, NM, May 1988, pp. 407-416.